

Article

Long-Term Thermo-Hydraulic Numerical Assessment of Thermo-Active Piles—A Case of Tropical Soils

Jiamin Zhang ¹, Daniel Dias ^{1,2}, Qiuqing Pan ^{3,*}, Chunjing Ma ¹ and Cristina de Hollanda Cavalcanti Tsuha ⁴¹ Université Grenoble Alpes, CNRS, Grenoble INP, 3SR, F-38000 Grenoble, France;

jiamin.zhang@3sr-grenoble.fr (J.Z.); daniel.dias@3sr-grenoble.fr (D.D.); chunjing.ma@3sr-grenoble.fr (C.M.)

² School of Automotive and Transportation Engineering, Hefei University of Technology, Hefei 230009, China³ School of Civil Engineering, Central South University, Hunan 410075, China⁴ Department of Geotechnical Engineering, University of São Paulo at São Carlos, Av. Trabalhador São-carlense, 400, São Carlos 13566-590, Brazil; chctsuha@sc.usp.br

* Correspondence: qiuqing.pan@csu.edu.cn

Abstract: Thermo-active piles are an upcoming technology for the utilization of subsurface geothermal energy in urban areas. This environmentally friendly technology has already been widespread for the heating and cooling of buildings in temperate regions, whereas in tropical regions it is still limited due to their unbalanced energy demands. This paper presents 3D thermo-hydraulic coupled numerical simulations to assess the long-term performance of thermo-active pile systems in tropical environments for different energy demands. The simulations are based on real data (in situ tests and field investigations) considering three typical thermal solicitations, thereby maintaining their practical relevance. Moreover, the energy exchange within soil control volumes is quantified based on an approach that allows calculating conductive and advective divergence. Parametric analyses regarding thermal solicitation, pile diameter, and groundwater flow are also performed. The results indicate that groundwater flow plays the most important role in improving the thermal balance of thermo-active piles.



Citation: Zhang, J.; Dias, D.; Pan, Q.; Ma, C.; Tsuha, C.d.H.C. Long-Term Thermo-Hydraulic Numerical Assessment of Thermo-Active Piles—A Case of Tropical Soils. *Appl. Sci.* **2022**, *12*, 7653. <https://doi.org/10.3390/app12157653>

Academic Editor: Andrea Frazzica

Received: 9 July 2022

Accepted: 27 July 2022

Published: 29 July 2022

Publisher's Note: MDPI stays neutral with regard to jurisdictional claims in published maps and institutional affiliations.



Copyright: © 2022 by the authors. Licensee MDPI, Basel, Switzerland. This article is an open access article distributed under the terms and conditions of the Creative Commons Attribution (CC BY) license (<https://creativecommons.org/licenses/by/4.0/>).

Keywords: thermo-active pile; tropical region; conduction; advection; temperature effects

1. Introduction

Heating and cooling demands account for most of the energy consumption of domestic and commercial buildings. Traditional solutions for heating and cooling buildings consume large amounts of electricity, natural gas, or fuel. According to REN21 (2022) [1], fossil fuel sources compose about 78.5% of the worldwide total energy consumption, whereas only 12.6% is generated from renewable energy sources. To lower the use of fossil fuels and develop greenhouse gases emission, the Ground Source Heat Pump (GSHP) systems, also known as geothermal energy systems, have been developed within the last few decades representing both environmentally and economically friendly solutions to fulfill the increasing energy demand.

Among various kinds of geostructures (piles, diaphragm walls, basement slabs or walls, barrettes, tunnel linings) in which heat exchanging pipes can be installed and act corporately in providing both structural and heat exchange purposes, thermo-active piles are the most widely applied and are the focus of this study [2–4]. As shown in Figure 1, piles inject heat into the soil at higher climate temperatures and extract heat from the ground at lower temperatures. The circulation of the heat exchange fluid is controlled by the heat pump.

Up to now, most of the existing thermo-active piles have been characterized by a temperate climate, where the ground temperature stays relatively constant between 10 °C and 15 °C over depths from 10 m to 50 m [5]. Whereas in tropical and hot dry climate zones, the energy demand for cooling is very important (around 56% of electricity consumption),

and heat is injected continuously into the ground due to the GSHP system operation. The use of thermo-active piles or geostructures systems may cause an increase in the ground temperature and then affect their long-term performance.

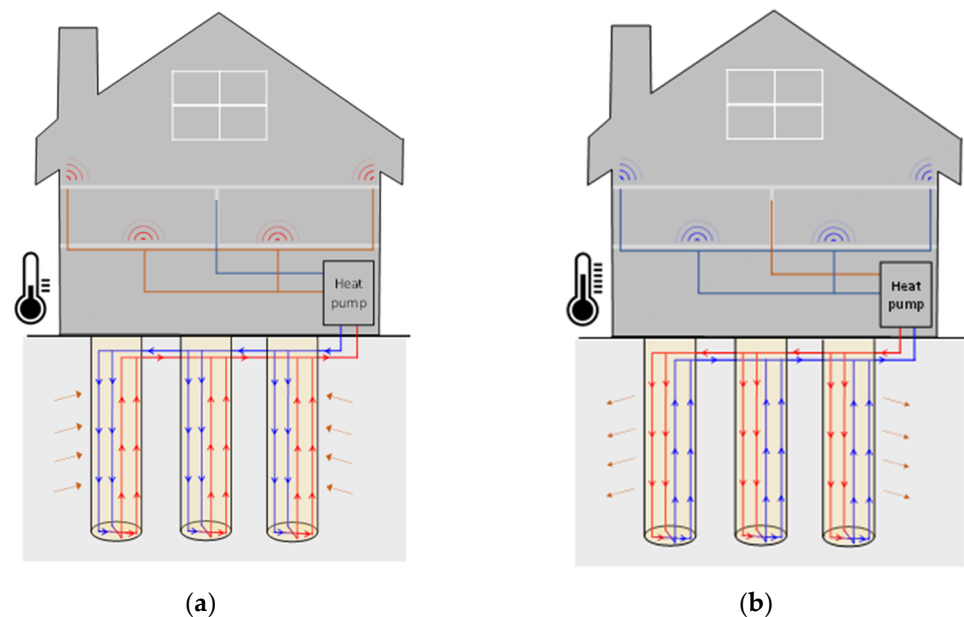


Figure 1. The application of thermal-active piles based on energy demand of building: (a) Heating mode, and (b) cooling mode.

Although the implementation of thermo-active piles/geostructures has been increasing rapidly, till now no common design codes and methodologies exist. Guidelines and recommendations for the design of thermo-active pile foundations can be found in Germany (VDI,2001) [6], Switzerland (SIA, 2005) [7], UK (NHBC, 2010) [8], and France (French Recommendations, 2016) [9]. The responses of thermo-active piles are highly affected by the applied thermal load, the ground conditions, the degrees of end restraints as well as pile characteristics (geometry and concrete elastic modulus) [10–12]. The main features caused by thermal solicitations of thermo-active piles are characterized by the axial deformation of the structure, the stress/load variations induced by the constrained thermal expansion and contraction, and the resistance changes resulting from heating and cooling [3,13].

The design approaches for thermos-active geosystems affected by groundwater flow have not been well defined yet. Therefore, analytical solutions for the ground temperature response functions based on the infinite line heat source approach are adopted in this work to assess heat transfer with the presence of groundwater flow [14]. Thermo-hydraulic coupled simulations can provide a more thorough understanding of the system temperature influence on the surrounding environment and heat diversion. In addition, the assessment of thermo-active system performance in various aspects such as the long-term heat exchange behavior is still an open issue.

The thermal operation of thermo-active structures strongly depends on the regional heating and cooling energy demands [15,16]. When they are nonsymmetrical over seasons, the sustainability will be directly affected, especially in tropical climates or cold regions. Sittidumrong et al. (2019) conducted oedometric tests regarding the tropical Bangkok sand. In this region, the ground temperature near the pile-soil interface can increase from 28–30 °C to 50 °C due to the thermo-active pile's operation [17]. Morais et al. (2020) performed a series of laboratory and field tests to evaluate the seasonal thermal performance of a thermo-active pile in a typical Brazilian tropical soil profile [18]. The studied unsaturated tropical soil thermal conductivity increases by 32% after the rainy season, leading to a heat transfer efficiency variation. It is also critical to evaluate the climatic temperature information, particularly in regions with inherent seasonal variability. Roy et al. (2020) investigated

the applications of thermo-active structures under tropical and subtropical climates in a commercial scope [19]. Compared to the subtropical regions, the thermo-active systems in tropical regions are less economically viable due to their inefficient performance and high cooling demand. The more balance between heating and cooling, the more economically feasible is the GSHP system. Casagrande et al. (2021) carried out thermal response tests on a thermo-active micropile in a typical tropical sedimentary stratified soil profile [20].

The long-term assessment of the thermal balance of the GSHP system provides implications for its thermal sustainability. However, most of the existing literature ignores this point. Rybach and Eugster (2010) experimentally and numerically demonstrated that single borehole heat exchanger-coupled geothermal heat pumps can operate sustainably for decades with combined heating and cooling demands [21]. For the long-term performance, Zanchini et al. (2012) used the finite-element method to investigate the role of groundwater flow on the 10-year performance of large borehole heat exchangers, it was shown that the groundwater flow does not affect the hourly peak thermal loads but improves the long-term system efficiency [22]. Bidarmaghz et al. (2016) studied numerically the effect of surface air temperature fluctuations on the GSHP heat exchange rate over 25 years, which would reduce the length of 30m-deep thermo-active piles by about 11% to achieve economic savings [23]. This effect was also emphasized by Choi et al. (2018) [24]. Iorio et al. carried out a numerical analysis to assess 60 years of thermal perturbation from a low enthalpy heating plant. They showed that sustainability is related to the characteristics of the groundwater flow (direction and pressure) and the position of the geothermal system [25].

The lack of knowledge of the long-term performance of thermo-active piles in tropical regions motivates this study. Differing from other studies conducted in temperate regions, tropical climatic temperatures and geological conditions are taken into account here, and energy demands in three cities in Brazil are chosen. This work also performed parametric analysis through coupling thermo-hydraulic numerical simulations. The thermal behaviors of a thermo-active pile for 10 years are investigated. Additionally, a numerical approach compiled in the FISH language is used to quantify the heat exchange in terms of conduction and advection, which distinguishes the contribution of groundwater flow and the ground. The distinction between conduction and advection divergence for the energy exchange with the presence of groundwater flow is therefore investigated. Some recommendations on the proper implantation conditions of thermo-active piles at the design stage are addressed at the end.

2. Numerical, Modeling of the Long-Term Performance of Thermo-Active Piles

2.1. Heat Transfer Mechanisms

Heat conduction mainly occurs within solid materials, such as the pile and the ground. It is governed by the material's thermal properties. The heat transfer driven by the groundwater flow and the heat exchange between circulating fluid and pipes are mainly controlled by the thermal convection mechanism. Generally, compared to the other two phenomena, radiation is negligible for heat transfer in a thermo-active pile system.

2.1.1. Heat Transfer between Thermo-Active Geostructures and Soil Masses

In soils, conduction is usually the dominant process, but if the groundwater flow is present, then advection can also be important [26]. In thermo-active piles, conduction takes place in the concrete and the pipe wall, while convection happens within the pipes owing to the internal flow of the heat transfer fluid. This study assumes that the heat transfer in thermo-active pile systems can be simplified into two phenomena: the pile-ground conduction and the groundwater flow carried advection.

To estimate the total thermal exchange between these two media, most existing studies use the following equation:

$$Q_{total} = m_f c_f (T_{in} - T_{out}) \quad (1)$$

where Q_{total} is the heat exchange (W), m_f is the mass flow rate of the heat carrier fluid (kg/s), c_f is the specific heat of the flowing fluid (J/kg/K), T_{in} and T_{out} (K) are respectively the fluid temperatures at inlet and outlet. Considering that the difference between inlet

and outlet temperatures is usually lower than 5 degrees, it approximates the total thermal transfer efficiency as a first approach. However, this approach can only assess the total heat exchange. Also, an average temperature is applied to the finite line heat sources (see Section 2.2.2). Therefore, a strategy developed by Rammal (2017) and Delerablée et al. (2018) to evaluate the conductive and advective heat exchange by thermo-active geostructures and the surrounding soil is adopted [27,28].

The energy balance equation can generally be expressed in its differential form, which represents the contribution of conduction and advection as:

$$C_{eff} \frac{\partial T}{\partial t} + \text{div} \left(\vec{J}_{cond} \right) + \text{div} \left(\vec{J}_{adv} \right) - j_{int} = 0 \quad (2)$$

where C_{eff} is the effective volumetric specific heat ($\text{J}/\text{m}^3/\text{K}$), T is the temperature (K), \vec{J}_{cond} is the conductive heat flux (W/m^2), \vec{J}_{adv} is the advective heat flux and j_{int} is the production of internal volumetric heat (W/m^3) which is normally ignored in terms of the limited depth of the structures and the geology.

$$C_{eff} = \rho_g c_g + n_g S \rho_w c_w \quad (3)$$

where S is the degree of saturation, n_g is the porosity, $\rho_g c_g$ and $\rho_w c_w$ are the volumetric specific heat of soil and water ($\text{J}/\text{kg}/\text{K}$), respectively.

This differential form of energy balance equation makes it possible to reveal the divergence of fluxes by conduction and advection in thermal transfers (depending on the presence or absence of groundwater flow). The conductive or advective divergence can be calculated at each instant for each solid element.

Thus, the divergence of the advective flux is defined by the following equation:

$$\text{div} \left(\vec{J}_{adv} \right) = \vec{\nabla} \cdot \vec{J}_{adv} = \vec{\nabla} \cdot \left(\rho_w c_w \vec{v}_D T_{(x,y,z)} \right) = \rho_w c_w \left(\vec{v}_D \cdot \vec{\nabla} T_{(x,y,z)} + T_{(x,y,z)} \vec{\nabla} \cdot \vec{v}_D \right) \quad (4)$$

where \vec{J}_{adv} is the vector of the advective term for each zone i and at each time t , ρ_w is the density of water (kg/m^3), c_w is the specific heat of the water ($\text{J}/\text{kg}/\text{K}$), \vec{v}_D is the fluid specific discharge (Darcy velocity in m/s), and $T_{(x,y,z)}$ is the zone temperature. Since the water is not compressible, the divergence of the Darcy velocity is zero, and the equation becomes:

$$\text{div} \left(\vec{J}_{adv} \right) = \rho_w c_w \vec{v}_D \cdot \vec{\nabla} T_{(x,y,z)} \quad (5)$$

Following Fourier's law, the divergence of the conductive flux is defined by:

$$\vec{J}_{cond} = -\lambda_{g,eff} \vec{\nabla} T_{(x,y,z)} \quad (6)$$

where \vec{J}_{cond} is the vector of the conductive term, $\lambda_{g,eff}$ is the element effective thermal conductivity ($\text{W}/\text{m}/\text{K}$).

$$\lambda_{g,eff} = \lambda_g + n_g S \lambda_w \quad (7)$$

where λ_g and λ_w is the thermal conductivity of soil and water, respectively ($\text{W}/\text{m}/\text{K}$), S is the degree of saturation and n_g is the porosity. All the thermal parameters refer to the bulk properties.

It should be noted that in this approach, heat exchange pipes are not modeled but replaced by equivalent line heat sources in the thermo-active piles, so the convective heat exchange for pipes is zero.

2.1.2. Thermal Exchange Power Evaluation

The flux-divergence theorem, also known as Ostrogradsky's theorem, states that the sum of all sources gives the net flux out of a region. According to the following formula, the advective and conductive flux is equal to the total heat exchange in the considered volume:

$$\iiint_V \vec{\nabla} \cdot \vec{q} dV = \iint_{S_{th}} \vec{q} \cdot \vec{n} dS \quad (8)$$

where V (m^3) is the volume of a body, $\vec{\nabla} \cdot \vec{q}$ is the divergence of the flux (W/m^3), \vec{q} is the flux density (W/m^2), \vec{n} is the flux vector and S_{th} is the heat exchange surface (m^2). In steady-state conditions, the equation becomes:

$$\iiint_V \vec{\nabla} \cdot \vec{q} dV = 0 \quad (9)$$

The divergence integration for the total volumetric thermal exchange $P_v(t)$ in a control volume V at the time t can be defined as:

$$P_v(t) = \sum_{i=1}^N V_i \left(\text{div} \left(\vec{J}_{adv,i}(t) \right) + \text{div} \left(\vec{J}_{cond,i}(t) \right) \right) \quad (10)$$

where $\text{div} \left(\vec{J}_{adv,i}(t) \right)$ and $\text{div} \left(\vec{J}_{cond,i}(t) \right)$ are the divergence of advection and conduction for each zone i and at each time t (s), N is the total number of the zones contained in the control volume.

Consequently, the corresponding energy (J) exchanged within the control volume for a certain period of time can be calculated by:

$$Q_v(t) = \sum_{i=1}^N V_i \left(\text{div} \left(\vec{J}_{adv,i}(t) \right) + \text{div} \left(\vec{J}_{cond,i}(t) \right) \right) \Delta t \quad (11)$$

where Δt stands for the duration of system operation.

2.2. Energy Demand Assessment

In temperate climates, buildings have relatively balanced needs for cooling and heating. When only cooling is required or when the energy demands are highly uneven, the thermal performance of the system may drop after a period. A thermal drift in the ground can then happen. Determining how much energy can be extracted or stored within the ground is an essential step to assure the efficiency of the system and restrict the temperature changes in the entire system. Climate and thermal regulations of the country/region are the main factors that affect the energy demand of buildings.

2.2.1. Climatic Conditions in Brazil

Brazil is the eighth-largest energy consumer throughout the world, with its vast tropical areas, the total primary energy consumption in Brazil has increased by 28% in the past decades due to economic growth [29]. The implementation of an efficient GSHP system would substantially reduce its primary energy consumption and carbon emissions. Several exploitations of the thermo-active geostructures were conducted in this region, but its application is still limited due to the scarcity of reliable thermal design approaches and poor understanding of its long-term thermo-hydraulic behavior in tropical regions. Anyhow, the Return On Investment (ROI) has to meet expectations in order to answer economic questions. Therefore, there is a strong interest in the assessment of the sustainability and efficiency of this technology in these regions [20].

Although most of Brazil lies in the tropics, the climatic conditions are various in cities due to its large country size. While in the northern cities of the Amazonas state (Manaus), the climate can get extremely hot all year. Cities such as São Paulo, Brasília and

Belo Horizonte have mild climates. The southern cities of Porto Alegre and Curitiba have mild winters. Therefore, three cities representing different corresponding regional climate characteristics are selected as the source of different thermal solicitations applied in this study: Brasilia, Porto Alegre, and Manaus (Figure 2).

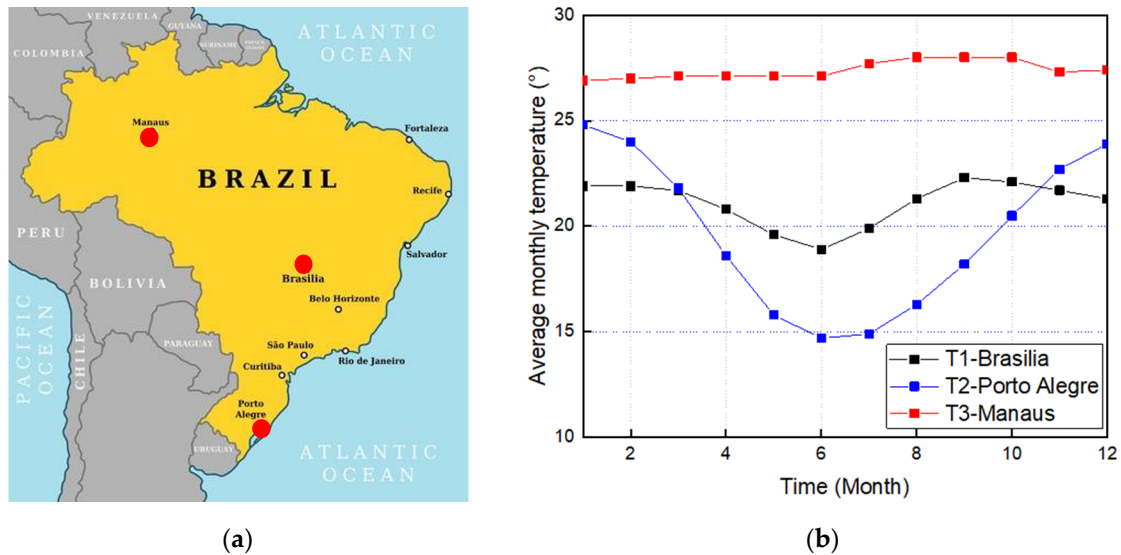


Figure 2. Locations (a) and the monitored monthly average temperature (b) of the three cities (<https://www.123rf.com>) (accessed on 9 July 2022).

The variation of ambient temperature in Brasilia can be described by a continuous sinusoidal curve:

$$T(t) = \bar{T}_{year} + A_T(\sin(\omega t) + \varphi) \quad (12)$$

where $T(t)$ is the instant temperature at the time t ($^{\circ}\text{C}$), \bar{T}_{year} is the annual average temperature which equals 20.7°C , $A_T = 1.79$ is the maximum annual amplitude, $\omega = 2.03 \times 10^{-7}$ is the radial frequency of the annual signal phase, and $\varphi = 2.11$ specifies where in its cycle the oscillation is at $t = 0$.

Considering the same sinusoidal form as in Brasilia, the real annual temperature variation in Porto Alegre can be converted into a more complicated curve:

$$T(t) = 5.16 \sin(2.05 \times 10^{-7} \cdot t + 1.39) + 0.04 \cos(0.5t + 80) + 19.54 \quad (13)$$

The temperature is relatively constant in Manaus with an average of 27.4°C .

2.2.2. Thermal Solicitations

Based on the real external air temperature variations in the three selected cities, three different types of thermal solicitations imposed on the piles can be derived: T1—Brasilia; T2—Porto Alegre; T3—Manaus. As shown in Table 1, about one-third of the time in a year in Brasilia, buildings need to be heated. Since the peak cooling power requirements can be considerably higher than the peak heating power requirements, a smaller amplitude was adopted for the heating phase [30]. The energy injected and extracted during the year is proportional to the duration of cooling and heating and maintains a balance of respectively 37 and 63%. In Porto Alegre, it is almost half for heating and half for cooling, while in Manaus the energy demand is 100% for cooling.

The heat exchangers (absorber tubes) are modeled by finite line heat sources (FLS) instead of applying heat flux boundaries in the pile to simulate the energy exchange. For feasibility studies and pre-design of energy foundations, the decision tree coming from the Swiss Society for Engineers and Architects (SIA) is used to define the FLS intensity of thermo-active pile foundations (Figure 3). It considers the operation mode of the

geothermal system as well as the ground conditions where the heat exchangers are installed, in particular the groundwater flow presence. In addition, the comfort air temperature threshold known from the Passivhaus standard (international energy performance standard for buildings) is assumed to be 20 °C. Therefore, when the temperature is above 20 °C, heat source power is positive, which means heat is injected into the ground to meet the cooling demand of buildings; while it is below 20 °C, the heat source power value is negative, allowing the pile to extract heat from the soil to meet the heating demand. Considering these factors, transient line heat source intensities of the whole energy pile for 1 year (1 cycle) are implemented in relation to the temperature and can be defined in Figure 4. As shown in this figure, three various typical tropical climate conditions are selected in this study: Manaus in the Amazonas state of Brazil with a constant high temperature of 27.4 °C, Brasilia with a mild climate zone with a temperature range of 18.9–22.5 °C. Porto Alegre in the south of the South American Plate with a temperature range of 14.4–24.7 °C. The magnitudes of their temperature variations are 0 °C, 3.6 °C, and 10 °C respectively.

The transient thermal power of T1 and T2 fall in the ranges of [−30, 45] W/m and [−45, 45] W/m, respectively (pile diameter is 1 m), with a negative sign representing heat exaction. For T3 the power is fixed at 45 W/m. Depending on the temperature variation, the energy injection or extraction of the pile will also change. The heating peak and cooling peak of the pile are donated by HP and CP, respectively. In real practice, energy injection and extraction will not very likely be proportional to the cooling and heating demands, however, to quantify and compare the impact of imbalanced thermal demands, the simplified design of thermal solicitations described above is adopted.

2.3. Ground Investigations

2.3.1. Tropical Soil Thermal Properties—In Situ Measurements (TRT)

As tropical weathering involves decomposition and chemical–mineralogical and structural transformation, tropical soils have different properties and behaviors from the soils in temperate/cold regions [31]. In Brazil, lateritic soils are abundant. They are the product of an intensive weathering called laterization. The recurrence of wet and dry seasons is an important feature of laterite formation. The laterization process is defined by the migration of particles through water infiltration, creating a highly porous layer with almost exclusively the most stable minerals (e.g., quartz and kaolinite) and enriching the soil with iron and aluminum and their associated oxides such as sesquioxide [32]. According to Vargas (1975), the lixiviation and particle cementation are responsible for the formation of aggregates and a porous structure, which generally results in a soil with an open structure, low specific gravity, high void ratio, high permeability, and high resistance to erosion [33]. The macro-porous structure makes these soils highly compressible, aside from usually exhibiting collapsible behavior.

Table 1. The assessment of heating and cooling demand over 1 year for the three types of thermal solicitations.

Parameters		T1—Brasilia	T2—Porto Alegre	T3—Manaus
Heating	Time [day]	133	187	-
	P_{max} [W/m]	30	45	-
Cooling	Time [day]	227	173	360
	P_{max} [W/m]	45	45	45
Imbalance	%	37–63	52–48	0–100

To choose the most appropriate sites for the implantation of thermo-active geostructures, the various thermal, hydraulic, and mechanical properties of sites should be taken into consideration. In terms of porosity, water content, hydraulic conductivity, density, deformability and strength, standard test methods are used for the quantification of these properties of soils. For their thermal properties, the “geothermal response test” is rec-

ommended. Thermal conductivity and volumetric heat capacity are the most significant thermal properties of soils which are crucial to an engineering design [34].

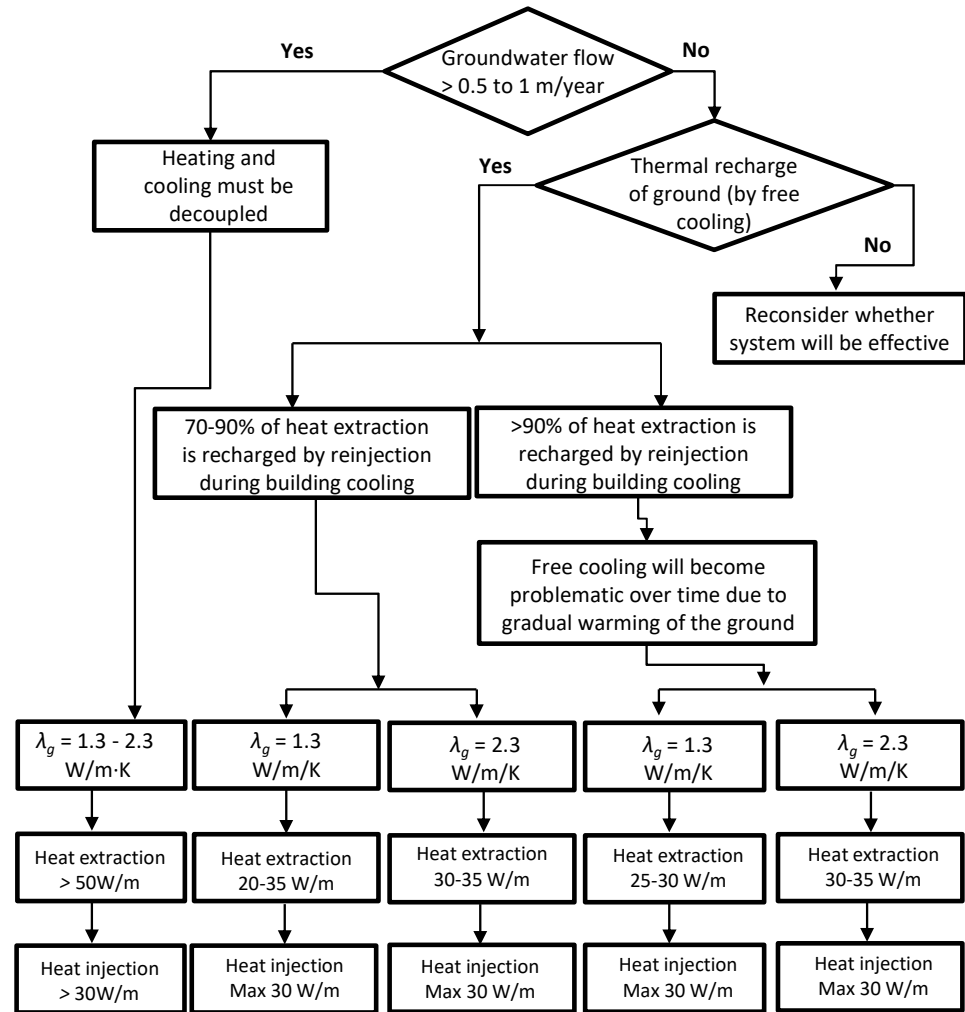


Figure 3. Flow chart for energy output for pile heat exchangers. Note: for piles greater than 0.4 m in diameter, the spacing is usually larger and the above performance can be improved upon, possibly by up to 50% for large (>1 m) diameters.

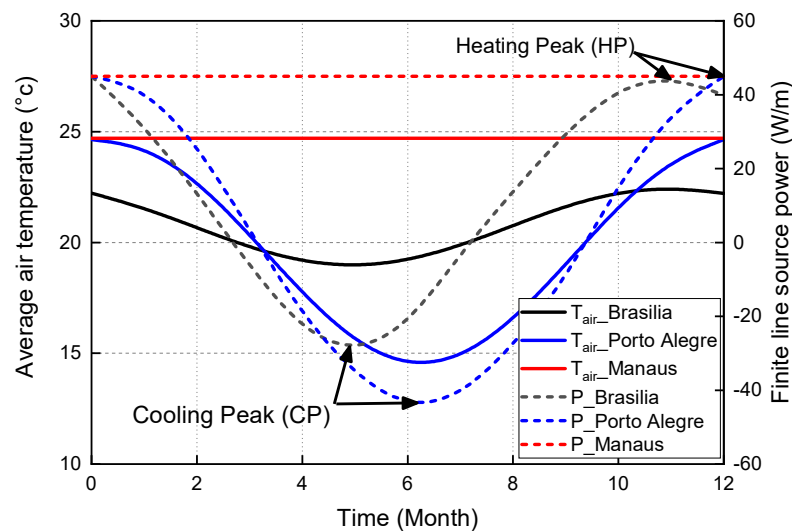


Figure 4. Annual ambient temperature and finite heat source power for three cities (1 year/1 cyclic).

A Thermal Response Test (TRT) was performed by Morais and Tsuha in Sao Paulo city [35]. It was carried out by injecting a constant heating power via the heat circulating fluid within a thermo-active micropile. The pile with a diameter of 0.35 m and a length of 15 m was equipped with a U-shaped pipe. During approximately 10 days of operation, the inlet fluid was fed at a constant flow rate of $3.52 \times 10^{-4} \text{ m}^3/\text{s}$ and the inlet temperature was monitored along with the outlet temperature. The site represents a saturated clayey sand condition of the Brazilian southeast region. The groundwater table varies seasonally from 2–3 m below the ground surface and was 1.9 m when the test was performed.

The TRT results were interpreted based on Kelvin's linear heat source theory. Parameters were derived from this test:

- The undisturbed ground temperature: 297.85 K,
- The effective thermal conductivity λ_{eff} : 2.82 W/m/K,
- The average pile thermal resistance R_b : 0.13 m·K/W.

It is important to know that such thermal response tests are not enough to determine the properties of soils. Still, the in-situ measurements have the advantage to be done in 'real conditions', the measured effective thermal conductivity is adopted in this study as a reference value in the following parametric studies. It is worth noting that this effective value is equivalent to sedimentary limestone [36]. According to the soil profile and the measured thermal conductivity value, the soil specific heat capacity c_g is estimated as 2200 J/kg/K based on the table of soil thermal and hydraulic properties from Riederer and Nguyen (2007) [37].

To verify the reliability of the properties adopted, numerical simulations of a TRT test performed considering another experimental site were compared, based on the in-situ results reported by Morais and Tsuha [38] (case of an unsaturated soil). The average of fluid temperature, i.e., $(T_{\text{in}} + T_{\text{out}})/2$, and the variation of the ambient temperature with time are selected as the thermal loads. Two monitoring points were located at a depth of 7.5 m, with a distance from the pile axis of 1 m and 2 m, respectively. As shown in Figure 5, the model with the above soil properties is able to accurately capture and replicate the soil temperature responses to the test and are therefore employed in this study.

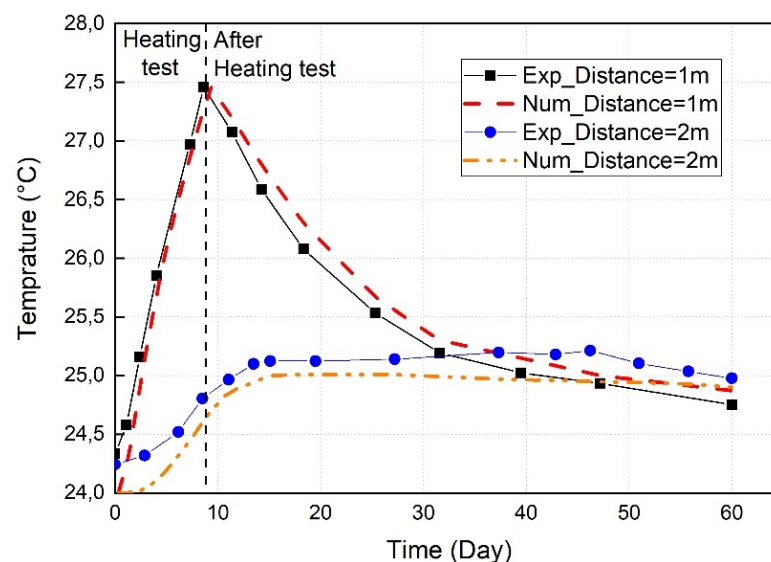


Figure 5. Comparison of the experimental and numerical ground temperature responses (at a distance of 1 m and 2 m from the pile axis) to the TRT.

2.3.2. Ground Temperature

In the design of thermo-active geostructures, the ground temperature is an influential factor. The daily ambient temperature variation cycles will affect the shallow ground temperature with a maximum depth of 10 m. The soil temperature remains constant at

depths greater than 10 m. Likewise, at greater depths well below 10 m downward, due to a small amount of heat being conducted from the earth towards the surface, the average temperature slightly increases with depth, the gradient is around 2.5 °C per 100 m.

The variation of ground temperature in the uppermost few meters forms a sinusoidal function as expressed in the following equation [39]:

$$T(z,t) = \bar{T}_{year} + A_T e^{-\left(\frac{z}{d}\right)} \left(\sin\left(\omega t + \varphi - \frac{z}{d}\right) \right) \tag{14}$$

where $T(Z,t)$ is the temperature at a depth z at an instant t (°C), ω is the radial frequency of the annual signal phase and d is the damping depth of the annual temperature signal (m) and is defined by $d = \sqrt{2\alpha/\omega}$, where α is the thermal diffusivity of the ground (m²/s), which can be obtained by $\alpha = \lambda/\rho c$. ρ is the density (kg/m³), λ is the thermal conductivity (W/m/K) and c is the heat capacity (J/kg/K).

Two of the three cases: T1—Brasilia and, T2—Porto Alegre, adopt this method to represent ground temperature. For T3—Manaus, the soil temperature is considered constant at all depths. According to the equations mentioned above, the calculated damping depths are presented in Table 2.

Table 2. Corresponding damping depths of the three cities.

City	T1—Brasilia	T2—Porto Alegre	T3—Manaus
Damping depth d [m]	2.36	1.37	-

Figure 6 presents a profile of the calculated variations of ground temperature with depth for T1—Brasilia. The difference between the surface temperatures is in the range of 3.5 to 10 °C, and the temperature convergence occurs at depths of 7 m for T1—Brasilia and 3 m for T2—Porto Alegre.

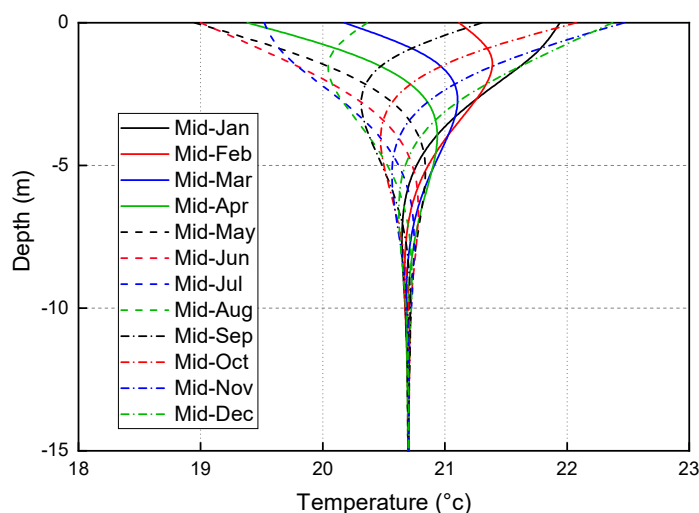


Figure 6. The variation of ground temperature with depths in Brasilia (T1).

2.3.3. Groundwater Conditions

In this work, hydrostatic and groundwater flow are considered. Based on the conditions of the in-situ TRT, the groundwater table is fixed at 2 m below the ground surface. The soil is considered dry above the groundwater table. When groundwater flow is present, the flow velocity is governed by Darcy’s law, which is related to the hydraulic gradient and the hydraulic conductivity. If the hydraulic gradient changes, the saturation zone will change, then the water content variation will significantly influence the thermal conductivity and the specific heat of soils. In this manner, different permeability values are selected to maintain the thermal properties of the medium in numerical calculations.

Note that since the water density and dynamic viscosity are assumed to be constant values in this study, and the flow rate is relatively large, the impact of temperature variation on groundwater flow can be neglected.

3. Results

3.1. Geometry and Boundary Conditions

The finite difference numerical analysis is conducted using the software FLAC^{3D} version 6.0. Unless otherwise stated, groundwater is considered to be static, and natural convection was not considered in this study. The top of the pile is suitably extended by 0.5 m to ensure that the temperature in pile head zones varies with the atmospheric temperature.

A thermo-active pile with a diameter of 1 m and a length of 9.5 m is set up in the soil mass. The soil properties are adopted from the TRT site. A monolayer is considered in order to reduce the calculation complexity, and its properties are assumed to be homogeneous as summarized in Table 3.

Table 3. The properties of the soil and the pile.

Material Properties	Units	Soil	Pile
Density, ρ	[kg/m ³]	2000	2500
Thermal conductivity, λ_{eff}	[W/m/K]	2.82	1.8
Specific heat capacity, c_p	[J/kg/K]	2200	1000
Hydraulic conductivity, k	[m/s]	1×10^{-6}	-
Saturation, S	-	1	-
Porosity, n	-	0.5	-

The finite line heat sources are applied at 10 cm from the pile-soil interface (see Figure 7), representing the real positions of the heat exchanger tubes. They are extruded along the full length of the considered piles, i.e., 9.5 m in this study. The heat power at each gridpoint is equal to $P(t)/2N$, $P(t)$ is the total thermal power of pile (W) and is given in Figure 4. Because only half of a pile is built, the simulated thermal power is also half of the total power and N is the number of all gridpoints that constitute the finite line source.

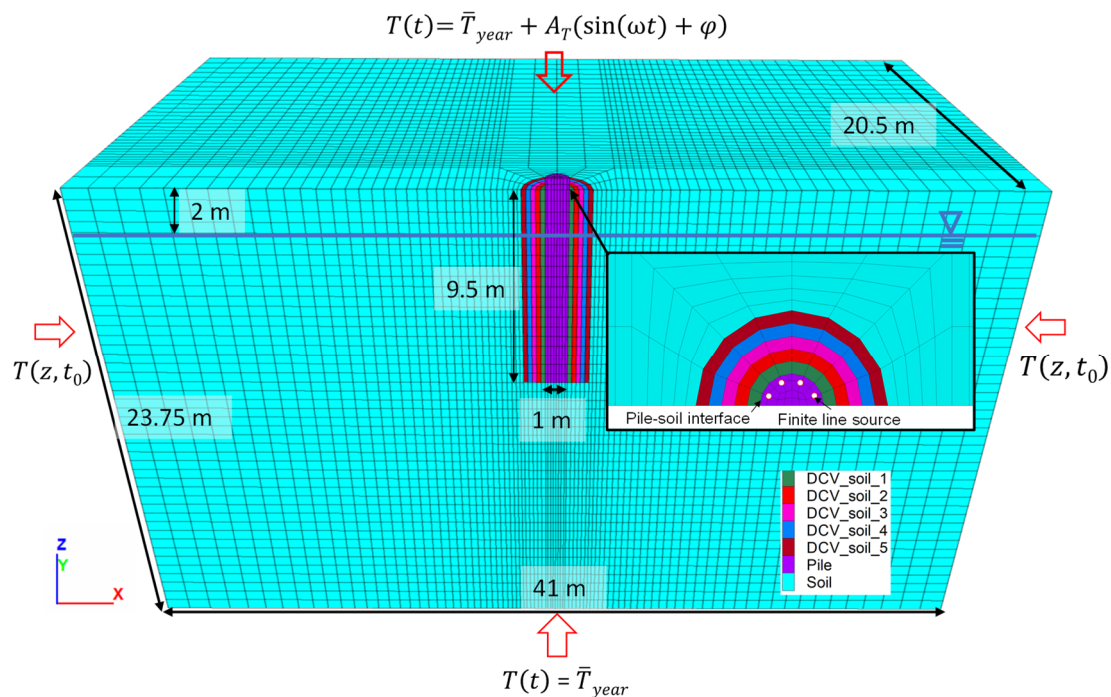


Figure 7. Geometry and boundary conditions of the 3D thermo-active pile numerical model.

A mesh refinement in the numerical analysis is considered at the pile proximity. A parametric analysis was conducted to determine the numerical model dimensions to avoid the boundary effects and to define adequate mesh refinement. The considered mesh (composed of 103,704 nodes) for the 3D model for the following analyses is shown in Figure 7.

3.2. Results and Discussions

3.2.1. Influence of Imposed Thermal Solicitation

Temperature variations at the pile-soil interface at different depths from the ground surface were measured. As shown in Figure 8, it reflects the long-term variation of the soil temperature at the pile vicinity. When the maximum and minimum temperatures at a specific position remain unchanged under the cyclic loading, thermal equilibrium is considered to be reached there. For better visualization, the maximum and minimum values for each year are connected by dashed lines. In the T1 case, minimum and maximum temperatures at three points increased rapidly in the first two years and then increased more slowly. The same increasing trend can be observed in the T3 case. It indicates that the average temperature around the pile is becoming less favorable to a cooling demand due to a residual ground temperature increase under these two thermal solicitations.

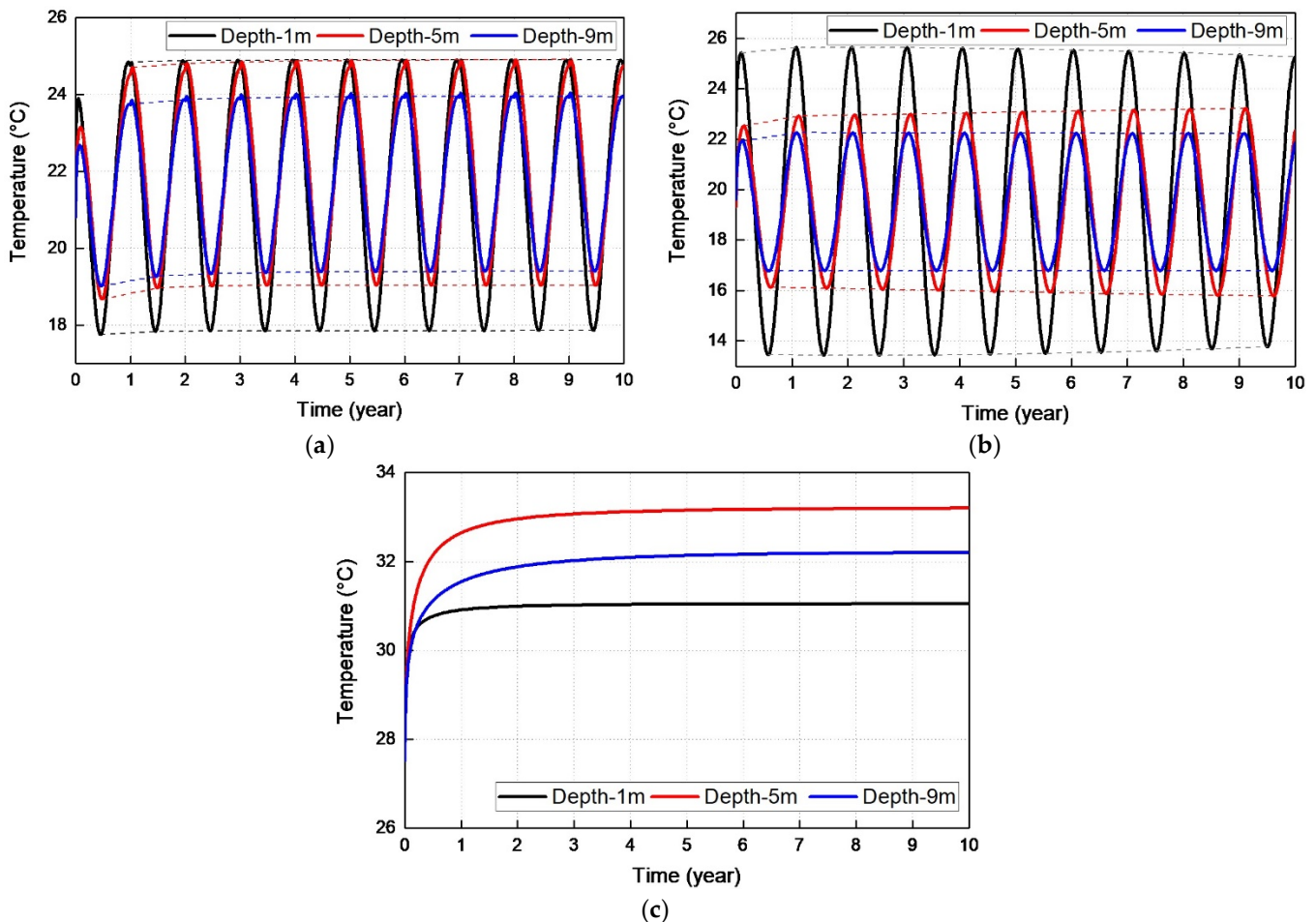


Figure 8. Comparison of temperatures at 1 m, 5 m, 9 m from the ground surface over 10 years of thermal solicitation for (a) T1—Brasilia, (b) T2—Porto Alegre and (c) T3—Manaus.

For the T2 case, the variation trends of the minimum and maximum temperatures are different for the three depths. The temperature change magnitude closer to the ground surface decreases from year to year, while the opposite trend is observed for the depth of 5 m. The difference between the minimum and maximum temperatures closer to the

pile bottom is basically constant for the depth of 9 m. The conclusion can be drawn that an accumulated temperature is induced in the middle part of the pile by the continuous cooling operation. The heat exchange in the pile head area is influenced by the ambient temperature and therefore counteracts part of the heat accumulation, and the temperature in the bottom part is lower than the middle due to a larger heat dissipation area. Unlike the other two thermal solicitations, the largest temperature change in T3 occurs at a depth of 5 m. The temperature change rate in these three thermal solicitations after 3 years shows that there is no significant degradation of the system sustainability over its entire service life (typically 30–50 years).

It is also important to note that the key to justifying the performance of thermo-active piles is to determine whether the building's demand for heating and cooling can be fulfilled without causing an important impact on themselves and their surroundings. The temperatures along the soil-pile interface to the model bottom at the heating peak and cooling peak in the last year are considered to represent the maximum values of each phase and are shown in Figure 9. The ISO 13256-1 standard recommends that the coefficient of performance (COP) must be higher than 3.3 and should be greater or equal to 4 for economic reasons [40]. To ensure this condition for the heating mode, the ground temperature should not be lower than 0 to 5 °C while the secondary circuit output temperature should not exceed 35 to 45 °C. The critical temperature threshold for the GSHP system is then defined between +1 °C and +35 °C [41].

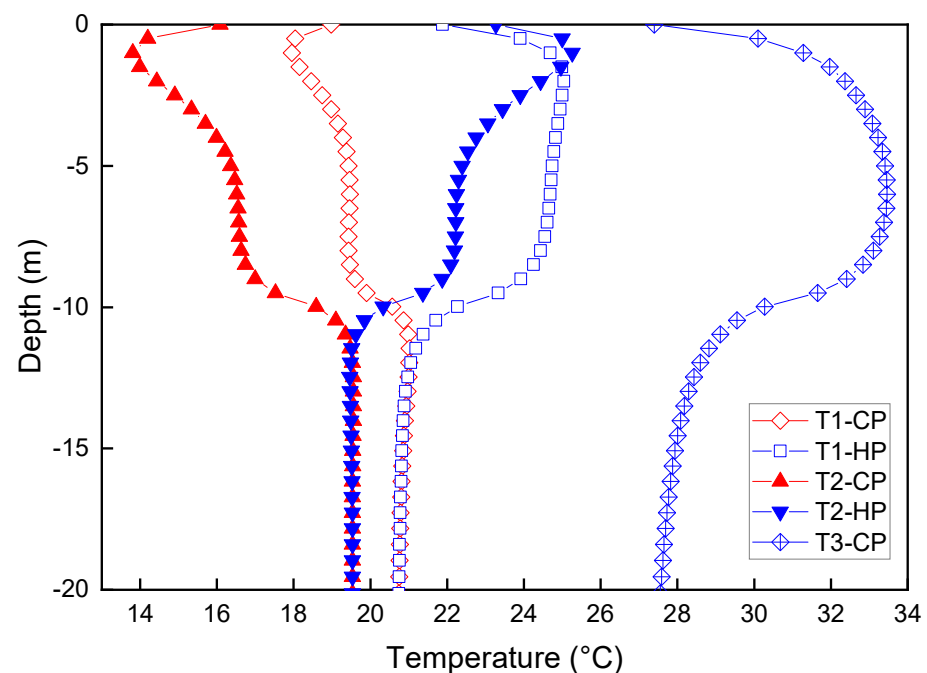


Figure 9. Temperatures of the pile-soil interface at heating and cooling peak for the 10th year for three thermal solicitations.

As shown in Figure 9, in the cases of T1 and T2, the maximum and minimum temperatures occur at the water table position. This is because the alternating operation of heating and cooling operations results in a smaller magnitude of accumulated temperature change around the pile with respect to the climate temperature. Therefore, the temperature in the area affected by air temperature is greater than in other parts of the pile, while the presence of groundwater increases the specific heat of the soil below the water table position, which is less affected by changes in air temperature. T3 is the most dangerous thermal operating mode, which causes a maximum accumulated temperature close to the temperature threshold. However, all temperatures fall within the limit range (1–35 °C) and ensure the functioning of the system.

The heat exchange per unit volume in different control volumes is quantified to obtain the heat inflow Q_{in} and heat outflow Q_{out} over a given operational cycle, which can be defined as follows:

$$Q_{in} = \left| \int_{\nabla T(x,y,z) > 0} P_v(t) dt \right| / V_c \quad (15)$$

$$Q_{out} = \left| \int_{\nabla T(x,y,z) < 0} P_v(t) dt \right| / V_c \quad (16)$$

where $\nabla T_{(x,y,z)}$ is the temperature difference compared to the last time step at the interest location ($^{\circ}\text{C}$). When it is lower than 0, the heat is considered to flow out of the zone. V_c is the control volume (m^3). The thermal balance in a control volume can be estimated as the difference between the heat inflow and the heat outflow. It represents the average heat loss (negative) or heat storage (positive) per unit control volume (kWh/m^3).

$$Q_{balance} = Q_{in} - Q_{out} \quad (17)$$

Figure 10 presents the average heat exchange per unit volume in different control volumes. As the distance against the pile-soil interface increases, Q_{in} and Q_{out} show a nonlinear decrease trend, and can be expressed by a quadratic equation. x corresponds to the distance between each control volume center and the pile-soil interface. Under the T1 thermal solicitation, the heat inflow of the 5 control volumes decreases by an average of 26% after 10 years and the heat outflow increases by an average of 30%, i.e., the heat injection capacity decreases but the heat extraction capacity increases. For T2, the heat injection capacity of the 5 control volumes after 10 years decreases by an average of 20% compared to the first year, while there is no significant change in heat outflow. T3 represents a continuous cooling demand, which does not include heat outflow throughout the year. After ten years of heat injection, the temperatures of the control volumes become stable, resulting in a smaller temperature change in the zones around the pile. The heat inflow after 10 years is less than 0.2% of the first year. Comparing these three different thermal solicitations, all operating modes show varying degrees of degradation in their capacities to meet the cooling demand after ten years. However, the performance of T2 is relatively better due to its balanced energy demands.

3.2.2. Influence of Pile Diameter

In this section, two other pile diameters are considered: $\varnothing = 0.7$ m and $\varnothing = 1.3$ m. A comparison is made concerning the reference case-T1 because this thermal solicitation can best represent the thermal operation under tropical conditions. Note that the dimension of the model changes with the pile diameter, since the length of the model is taken to be 41 times the pile diameter. The temperature distributions after 10 years are given in Figure 11. There is a relatively large temperature gradient around the pile with a smaller pile diameter. Although the pile diameter variation changes the layout of the line heat sources, it does not affect the ground thermal disturbance range. Only the pile body temperature is modified.

The variation of the average temperature of the pile over 10 years in Figure 12 shows that thermal equilibrium is achieved after the 2nd year for three diameters. The maximum and minimum values for each year are connected by dashed lines. Compared with the reference case, the pile volume is reduced by 51% for 0.7 m diameter and increased by 69% for 1.3 m diameter. Meanwhile, the maximum and minimum average pile body temperatures for 0.7 m diameter have increased by about 3.4% and decreased by 2.2% for 1.3 m diameter, respectively. Maintaining the density of the line heat source, change in the pile diameter, and the location of the line heat source have little effect on the long-term thermal performance of the system.

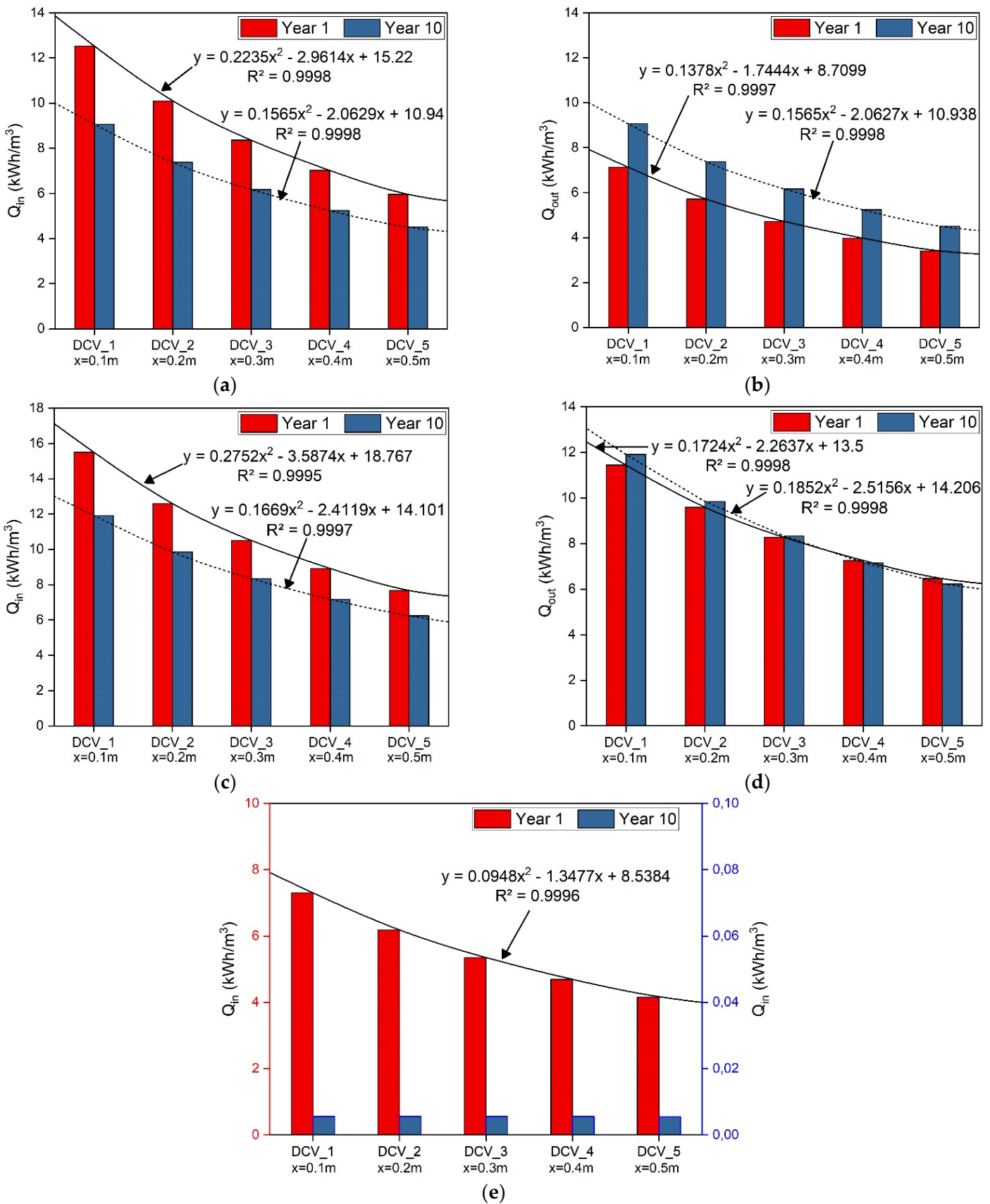


Figure 10. Heat exchange per unit control volume for different thermal solicitations: (a) T1-Q_{in}, (b) T1-Q_{out} (c) T2-Q_{in}, (d) T2-Q_{out} and (e) T3-Q_{in}.

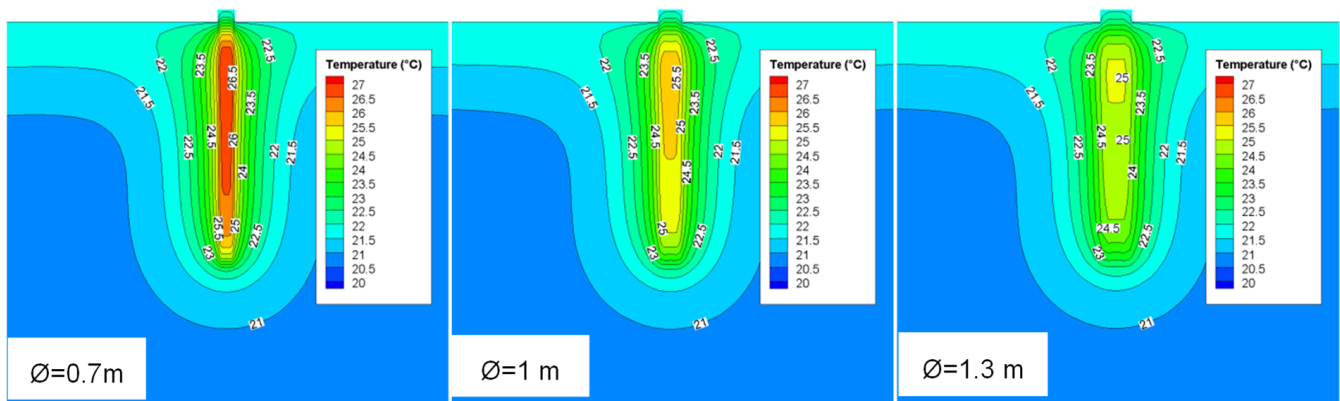


Figure 11. Temperature profiles around the pile with different diameters after 10 years of T1 thermal solicitation.

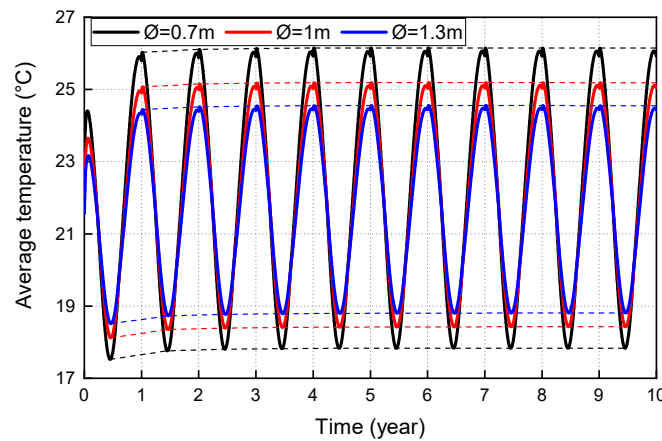


Figure 12. The variation of average pile body temperatures over 10 years for three pile diameters.

3.2.3. Influence of Groundwater Flow

The presence and movements of the groundwater can greatly influence the performance of thermo-active geostructures. Fromentin et al. (1997) show that when the velocity of groundwater flow is in the range from $1e-6$ to $1e-4$ m/s, the groundwater flow has a non-negligible influence on the heat transfer of thermo-active piles [36]. Di Donna et al. (2016) have also investigated the influences of groundwater flow velocity and of several other parameters on the heat exchange by conducting a numerical analysis [2]. When the groundwater flow is present, with an increase from 0 to 2 m/day, the exchanged heat improves by a factor of 3 to 8 times compared to the case without groundwater.

In the summer heat injection period, the surrounding soil around the pile may trap heat. By dissipating the high temperature elsewhere where the soil temperature is lower, the groundwater flow could be favorable [42]. This can eventually result in a steady condition and ensure the system performance. The phenomenon, named natural thermal recharging or natural thermal recovery, corresponds to extracting the heat injected in summer to meet the heating demand during winter and vice versa. It is worth mentioning that soils with high groundwater flow (up to $1e-6$ m/s) can produce natural heat regeneration [37].

The impact of groundwater flow is then discussed in this section, three groundwater flow velocities are considered: $v_D = 0$ m/day, 0.1 m/day, and 1 m/day. The thermal solicitation of T1- Brasilia is adopted for all the cases with a pile diameter of 1 m.

It can be seen in Figure 13a that the pile circular geometry slightly affects the groundwater flow velocity around the pile in the surrounding soil, creating an asymmetric form around the pile-soil interface. Compared to the average flow velocity, the flow velocities on the pile upstream and downstream sides are small, while there is an increase in flow

velocity near the tangency point of the pile-soil interface. Due to the advective heat transfer, asymmetry is also found in the temperature field (Figure 13b,c). A thermal plume is developed downstream of the pile and is maintained during the thermal solicitation cycles. The dissipation of energy leads to a moving thermal front whose velocity is proportional to the flow velocity.

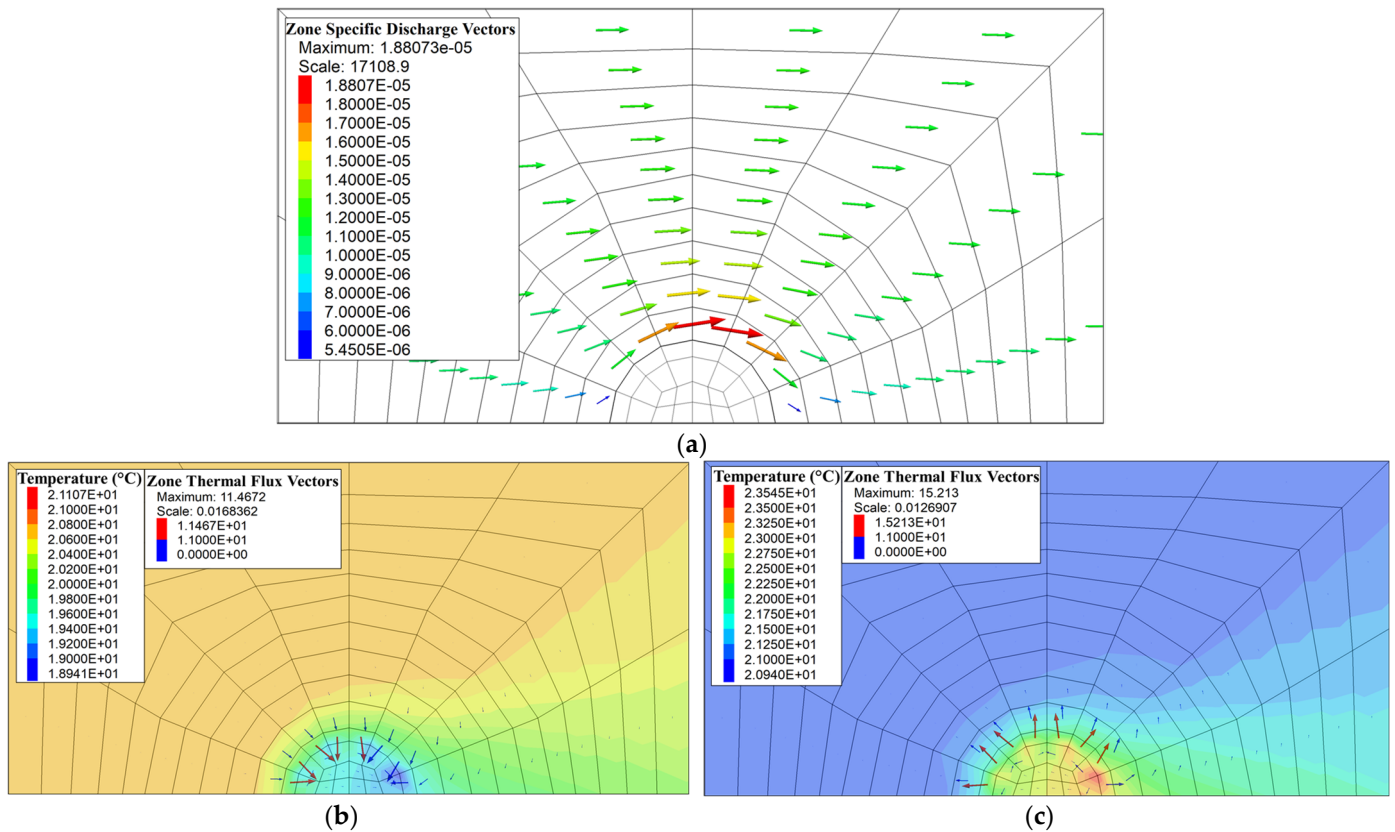


Figure 13. Thermal and hydraulic results around the pile after 10 years for $v_D = 1$ m/day: (a) Groundwater flow vectors, (b) heat flux vectors and temperature profile at cooling peak, and (c) heat flux vectors and temperature profile at heating peak.

The average temperature of the pile-soil interface reached thermal equilibrium at the end of the 1st year, except for the case of $v_D = 0$ m/day (Figure 14a), which implies even a small velocity of water flow can bring the pile temperature to thermal equilibrium quickly. The fluctuation range of average temperature is also reduced with the increase of water flow velocity. To better define the relationship between the average pile temperature fluctuation range after thermal equilibrium and the groundwater velocity, cases with $v_D = 0.25$ m/s, $v_D = 0.5$ m/s, $v_D = 0.75$ m/s are presented. As shown in Figure 14b, a nonlinear relationship is observed and the fluctuation range for the pile-soil interface temperature follows the same trend. Compared to the case of $v_D = 0$ m/day, the fluctuation range of average temperature decreases by about 45% for the pile and 55% for the pile-soil interface in the case of $v_D = 1$ m/day. It implies that the groundwater flow significantly reduces the pile thermal disturbance induced by the thermal operation, improving the pile thermal sustainability.

Table 4 visually quantifies the degradation in heat transfer capacity for different control volumes after 10 years. The energy exchanged induced by conduction and advection per unit of the control volume is denoted by Q_{cond} and Q_{adv} , respectively. With the increase of groundwater flow velocity, the energy exchanged by conduction decreases slightly but increases significantly by advection. In DCV_1, the total amount of energy exchange (sum of Q_{in} and Q_{out}) at 0.1 m/day groundwater flow velocity is 68% higher than the 0 m/day

one in the first year, and 585% higher when the water flow velocity is equal to 1 m/day. Due to the relatively large velocity of water flow near the pile, the DCV_1 also has the largest proportion of energy exchanged in advection to the total energy exchanged.

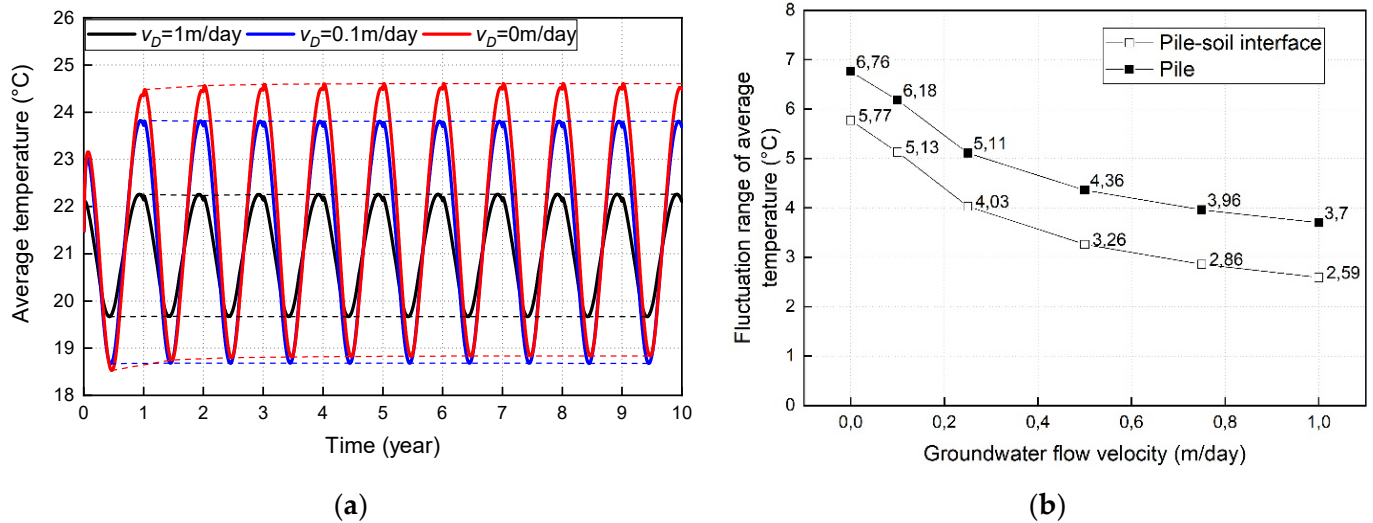


Figure 14. (a) Average temperature of the pile-soil interface over 10 years, and (b) fluctuation range of average temperature of pile-soil interface and pile for different groundwater flow velocities.

Table 4. The energy exchanged in the control volumes for different groundwater flow velocities in year 1 and year 10.

Time	v_D (m/day)	$Q_{in/out}$	Energy Exchanged (kWh/m ³)									
			DCV_1		DCV_2		DCV_3		DCV_4		DCV_5	
			Q_{cond}	Q_{adv}	Q_{cond}	Q_{adv}	Q_{cond}	Q_{adv}	Q_{cond}	Q_{adv}	Q_{cond}	Q_{adv}
Year 1	0	Q_{in}	12.52	-	10.11	-	8.36	-	7.02	-	5.96	-
		Q_{out}	7.13	-	5.72	-	4.72	-	3.98	-	3.41	-
	0.1	Q_{in}	11.05	10.53	8.57	8.11	6.89	5.87	5.69	4.09	4.82	2.81
		Q_{out}	6.74	4.64	5.22	3.66	4.20	2.77	3.49	2.07	2.98	1.57
Year 10	0	Q_{in}	4.60	90.10	2.84	30.16	2.15	6.68	1.81	2.68	1.60	1.46
		Q_{out}	3.26	36.62	2.11	12.59	1.66	3.19	1.44	1.60	1.31	1.14
	0.1	Q_{in}	9.06	-	7.38	-	6.17	-	5.24	-	4.51	-
		Q_{out}	9.06	-	7.38	-	6.17	-	5.24	-	4.51	-
1	Q_{in}	8.00	13.14	6.25	10.29	5.08	7.71	4.25	5.66	3.63	4.15	
	Q_{out}	8.00	4.80	6.25	3.73	5.08	2.77	4.25	2.02	3.63	1.49	

Compared to the first year, the energy exchange capacity in terms of conduction decreases in the 10th year in all control volumes. When water flow velocity is 0 m/day, a 7.8% reduction in DCV_1 and a 3.7% reduction in DCV_5 can be observed. Although a higher water flow reduces the conductive energy exchange capacity more importantly (12.8% reduction for $v_D = 1$ m/day), the total energy exchange amount increased slightly in some cases, indicating that the groundwater not only maintained the high energy exchange performance of the soil around the pile but even improved it.

It is noteworthy that the thermal solicitation of T1 refers to an energy demand dominated by cooling mode. Herein, the thermal balances of the 1st year and the 10th year in different control volumes shown in Figure 15 are positive. As the distance from the

pile-soil interface increases, the thermal balance decreases. It indicates a diminution of the thermal disturbance in the surrounding soil. The thermal balance in DCV_5 is reduced by 98.9% compared to DCV_1 with $v_D = 1$ m/day in the 10th year. This value is equal to 68% for $v_D = 0.1$ m/day. The heat was driven by a greater groundwater flow velocity to a wider range, thereby resulting in a smaller temperature difference around the pile. At the pile-soil interface (DCV_1), the temperature fluctuation range at $v_D = 1$ m/day is half of the $v_D = 0.1$ m/day one (2.59 °C vs. 5.13 °C, Figure 14b), while the groundwater flow velocity is 10 times higher than the $v_D = 0.1$ m/day one. The difference in $Q_{balance}$ is significant. On the contrary, in the control volume further away from the pile-soil interface (DCV_5), the groundwater flow velocity ratio remains constant, but the temperature variations induced by the heat source at $v_D = 1$ m/day drop drastically, leading to a small $Q_{balance}$.

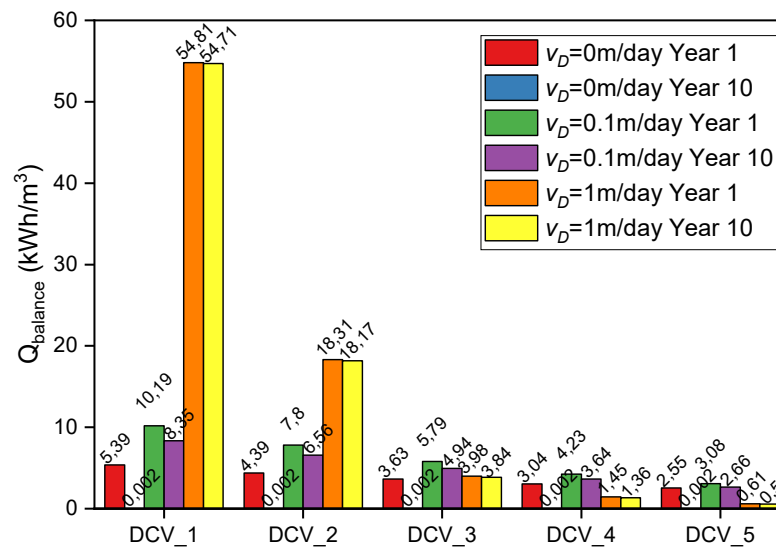


Figure 15. The thermal balance of the control volumes in the 1st year and 10th year for different groundwater flow velocities.

Meanwhile, the difference between the thermal balances of the 1st and 10th year decreases as the groundwater flow velocity increases. As the energy exchanged in the soil dissipates with the high-velocity water flow, the heat exchange capacities of the control volumes remain almost unchanged.

Under the combination of various conditions, the presence of groundwater flow is favorable to the heat transfer of the geothermal pile system thanks to the natural thermal recharge effect and the heat dissipation downstream. For the design of such structures in tropical regions, it is then possible to increase the cooling operation in situations where the groundwater flow is present. At the same time, if consideration is given to the impact on the pile group, the range of thermal disturbance will increase and may affect the performance of piles at the downstream side of the thermo-active pile, thus causing unfavorable additional thermal (including induced mechanical) loads. This needs to be studied alongside specific field cases. Theoretical development must take into consideration of the above factors prior to its application.

4. Conclusions

This work focuses on the long-term numerical assessment of a thermo-active pile in the tropical region by conducting 3D thermo-hydraulic coupled simulations using the finite difference method (FDM). The model parameters are based on in-situ results which therefore ensure its reliability. The numerical simulation permits to analyze the behavior of thermo-active piles in terms of temperature, and energy exchange of the selected control volumes. Parametric analysis of thermal solicitation and pile diameter as well as groundwater flow was performed.

In tropical regions, the thermal solicitation T3 (continuous cooling mode) would be ideal, but also the most dangerous demand. Compared to T1 and T2, it leads to a higher accumulated soil temperature. However, the maximum soil temperature around the pile in the studied cases does not exceed the threshold (35 °C). For T1 and T2, the maximum accumulated temperature occurs at the water table position, while T3 is around the pile center.

The energy exchange per unit of soil control volumes around the pile can be predicted by distance functions. After 10 years, the average soil heat injection around the pile decreased by 26% for the T1 thermal solicitation, but the heat extraction increased by 30%. While the heat injection decreased by 20% for T2, with no significant change in the heat extraction. The heat injection after 10 years is only 0.2 % of the 1st year for T3.

Variation of the pile diameter and pipe arrangement does not affect the thermal disturbance range under the T1 thermal solicitation but affects the pile average temperature.

A groundwater flow allows improving the thermo-active pile thermal sustainability. High groundwater flow velocity can nonlinearly reduce the average temperature of the pile-soil interface and pile body. Compared to $v_D = 0$ m/day, the average heat transfer per unit of soil control volumes increases about 6 times for $v_D = 1$ m/day. The thermal equilibrium in the 1st and 10th year remains quasi-constant for $v_D = 1$ m/day.

Extensive studies should be conducted to better understand the thermo-active piles' performance when applied in tropical regions. More particularly, the interaction between the thermo-active pile groups cannot be ignored, considering the conversion efficiency of the entire system scale rather than one single functioning pile will allow to quantify its performance more precisely.

Author Contributions: Conceptualization, J.Z. and D.D.; methodology, D.D.; software, J.Z.; validation, D.D., Q.P., C.M. and C.d.H.C.T.; formal analysis, J.Z. and D.D.; investigation, J.Z., Q.P., C.M. and D.D.; resources, D.D. and C.d.H.C.T.; data curation, J.Z., Q.P., C.M. and D.D.; writing—original draft preparation, J.Z.; writing—review and editing, D.D., Q.P., C.M.; visualization, J.Z., D.D., Q.P., C.M. and C.d.H.C.T.; supervision, D.D. and C.d.H.C.T.; project administration, D.D. and C.d.H.C.T.; funding acquisition, J.Z. and D.D. All authors have read and agreed to the published version of the manuscript.

Funding: This research was funded by China Scholarship Council, grant number 201908070075 and the laboratory 3SR is part of the LabEx Tec 21 (Investissement d'avenir—grant agreement no. ANR-11-LABX-0030).

Institutional Review Board Statement: Not applicable.

Informed Consent Statement: Not applicable.

Data Availability Statement: Not applicable.

Conflicts of Interest: The authors declare no conflict of interest.

References

1. REN21. *Renewables 2022 Global Status REPORT (GSR)*; REN21: Paris, France, 2022.
2. Di Donna, A.; Rotta Loria, A.F.; Laloui, L. Numerical Study of the Response of a Group of Energy Piles under Different Combinations of Thermo-Mechanical Loads. *Comput. Geotech.* **2016**, *72*, 126–142. [[CrossRef](#)]
3. Mohamad, Z.; Fardoun, F.; Meftah, F. A Review on Energy Piles Design, Evaluation, and Optimization. *J. Clean. Prod.* **2021**, *292*, 125802. [[CrossRef](#)]
4. Cecinato, F.; Salciarini, D. Energy Performance Assessment of Thermo-Active Micro-Piles via Numerical Modeling and Statistical Analysis. *Geomech. Energy Environ.* **2022**, *29*, 100268. [[CrossRef](#)]
5. Brandl, H. Energy Foundations and Other Thermo-Active Ground Structures. *Geotechnique* **2006**, *56*, 81–122. [[CrossRef](#)]
6. VDI. *Utilization of the Subsurface for Thermal Purposes—Underground Thermal Energy Storage*; Beuth Verlag GmbH: Berlin, Germany, 2001.
7. SIA. *Nutzung Der Erdwärme Mit Fundationspfählen Und Anderen Erdberührten Betonbauteilen*. Schweizer Ingenieur Und Architektenverband; SIA: Zürich, Switzerland, 2005.
8. National House Building Council (NHBC). *Efficient Design of Piled Foundations for Low Rise Housing, Design Guide*; NHBC: Milton Keynes, UK, 2010.

9. French Recommendations. *Recommandations Pour La Conception, Le Dimensionnement et La Mise En Oeuvre Des Géostructures Thermiques*. *Rev. Fr. Geotech.* **2016**, *1*, 149. [[CrossRef](#)]
10. Alberdi-Pagola, M.; Poulsen, S.E.; Jensen, R.L.; Madsen, S. Thermal Design Method for Multiple Precast Energy Piles. *Geothermics* **2019**, *78*, 201–210. [[CrossRef](#)]
11. Sterpi, D.; Angelotti, A.; Habibzadeh-Bigdarvish, O.; Jalili, D. Assessment of Thermal Behaviour of Thermo-Active Diaphragm Walls Based on Monitoring Data. *J. Rock Mech. Geotech. Eng.* **2018**, *10*, 1145–1153. [[CrossRef](#)]
12. Cunha, R.P.; Bourne-Webb, P.J. A Critical Review on the Current Knowledge of Geothermal Energy Piles to Sustainably Climatize Buildings. *Renew. Sustain. Energy Rev.* **2022**, *158*, 112072. [[CrossRef](#)]
13. Saggiu, R. Cyclic Pile-Soil Interaction Effects on Load-Displacement Behavior of Thermal Pile Groups in Sand. *Geotech. Geol. Eng.* **2022**, *40*, 647–661. [[CrossRef](#)]
14. Cherati, D.Y.; Ghasemi-Fare, O. Practical Approaches for Implementation of Energy Piles in Iran Based on the Lessons Learned from the Developed Countries Experiences. *Renew. Sustain. Energy Rev.* **2021**, *140*, 110748. [[CrossRef](#)]
15. Olgun, C.G.; Ozudogru, T.Y.; Abdelaziz, S.L.; Senol, A. Long-Term Performance of Heat Exchanger Piles. *Acta Geotech.* **2015**, *10*, 553–569. [[CrossRef](#)]
16. Santos Sá, L.M.; Hernandez Neto, A.; Tsuha, C.D.H.C.; Pessin, J.; Freitas, M.C.D.; Morais, T.D.S.O. Thermal Design of Energy Piles for a Hotel Building in Subtropical Climate: A Case Study in São Paulo, Brazil. *Soils Rocks* **2022**, *45*.
17. Sittidumrong, J.; Jotisankasa, A.; Chantawarangul, K. Effect of Thermal Cycles on Volumetric Behaviour of Bangkok Sand. *Geomech. Energy Environ.* **2019**, *20*, 100127. [[CrossRef](#)]
18. Morais, T.D.S.O.; Tsuha, C.D.H.C.; Neto, L.A.B.; Singh, R.M. Effects of Seasonal Variations on the Thermal Response of Energy Piles in an Unsaturated Brazilian Tropical Soil. *Energy Build.* **2020**, *216*, 109971. [[CrossRef](#)]
19. Roy, D.; Chakraborty, T.; Basu, D.; Bhattacharjee, B. Feasibility and Performance of Ground Source Heat Pump Systems for Commercial Applications in Tropical and Subtropical Climates. *Renew. Energy* **2020**, *152*, 467–483. [[CrossRef](#)]
20. Casagrande, B.; Saboya, F.; McCartney, J.S.; Tibana, S.; Saboya, F., Jr.; McCartney, J.S.; Tibana, S. Investigation of a Field-Scale Energy Micropile in Stratified Soil under Cyclic Temperature Changes. *Geomech. Energy Environ.* **2021**, *29*, 100263. [[CrossRef](#)]
21. Rybach, L.; Eugster, W.J. Sustainability Aspects of Geothermal Heat Pump Operation, with Experience from Switzerland. *Geothermics* **2010**, *39*, 365–369. [[CrossRef](#)]
22. Zanchini, E.; Lazzari, S.; Priarone, A. Long-Term Performance of Large Borehole Heat Exchanger Fields with Unbalanced Seasonal Loads and Groundwater Flow. *Energy* **2012**, *38*, 66–77. [[CrossRef](#)]
23. Bidarmaghz, A.; Narsilio, G.A.; Johnston, I.W.; Colls, S. The Importance of Surface Air Temperature Fluctuations on Long-Term Performance of Vertical Ground Heat Exchangers. *Geomech. Energy Environ.* **2016**, *6*, 35–44. [[CrossRef](#)]
24. Choi, W.; Ooka, R.; Nam, Y. Impact of Long-Term Operation of Ground-Source Heat Pump on Subsurface Thermal State in Urban Areas. *Sustain. Cities Soc.* **2018**, *38*, 429–439. [[CrossRef](#)]
25. Iorio, M.; Carotenuto, A.; Corniello, A.; Di Fraia, S.; Massarotti, N.; Mauro, A.; Somma, R.; Vanoli, L. Low Enthalpy Geothermal Systems in Structural Controlled Areas: A Sustainability Analysis of Geothermal Resource for Heating Plant (the Mondragone Case in Southern Appennines, Italy). *Energies* **2020**, *13*, 1237. [[CrossRef](#)]
26. Lou, Y.; Fang, P.; Xie, X.; Chong, C.S.A.; Li, F.; Liu, C.; Wang, Z.; Zhu, D. Numerical Research on Thermal Response for Geothermal Energy Pile Groups under Groundwater Flow. *Geomech. Energy Environ.* **2021**, *28*, 100257. [[CrossRef](#)]
27. Rammal, D. Thermo-Mechanical Behaviour of Geothermal Structures: Numerical Modelling and Recommendations. 2017. Available online: <https://www.theses.fr/2017LIL10172> (accessed on 9 July 2022).
28. Delerablée, Y.; Rammal, D.; Mroueh, H.; Burlon, S.; Habert, J.; Froitier, C. Integration of Thermoactive Metro Stations in a Smart Energy System: Feedbacks from the Grand Paris Project. *Infrastructures* **2018**, *3*, 56. [[CrossRef](#)]
29. US EIA. *International Energy Outlook 2019*; US EIA: Washington, DC, USA, 2019.
30. Loveridge, F. The Thermal Performance of Foundation Piles Used as Heat Exchangers in Ground Energy Systems. Ph.D. Thesis, University of Southampton, Southampton, UK, 2012.
31. De Carvalho, J.C.; de Rezende, L.R.; Cardoso, F.B.D.F.; Lucena, L.C.D.F.L.; Guimarães, R.C.; Valencia, Y.G. Tropical Soils for Highway Construction: Peculiarities and Considerations. *Transp. Geotech.* **2015**, *5*, 3–19. [[CrossRef](#)]
32. Rocha, B.P.; Pedrini, R.A.A.; Giacheti, H.L. Go/N Ratio in Tropical Soils from Brazil. *Electron. J. Geotech. Eng.* **2015**, *20*, 1915–1933.
33. Vargas, M. Structurally Unstable Soils in Southern Brazil: Conference. Session Four. 11F, 2T, 4R. PROC. EIGHTH INT. CONF. ON SOIL MECH. FOUND. ENGG, MOSCOW, V2. 2, 1973, P239–246. In *International Journal of Rock Mechanics and Mining Sciences & Geomechanics Abstracts*; Elsevier: Pergamon, Turkey, 1975; Volume 12, p. 54.
34. Ground Source Heat Pump Association. *GSHP Thermal Pile Design, Installation and Materials Standards*; Ground Source Heat Pump Association: London, UK, 2012.
35. Morais, T.d.S.O.; Tsuha, C.d.H.C. In-Situ Measurements of the Soil Thermal Properties for Energy Foundation Applications in São Paulo, Brazil. *Bulg. Chem. Commun.* **2018**, *50*, 34–41.
36. Fromentin, A.; Pahud, D.; Jacquier, C.; Morath, M. *Recommandations Pour La Réalisation d'Installations Avec Pieux Échangeurs. Empfehlungen für Energiepfahlssysteme*; SUPSI: Manno, Switzerland, 1997.
37. Riederer, P.; Nguyen, B. *Analyse Technico-Commerciale de Bâtiments Equipés de Fondations Géothermiques*; 2007.
38. Morais, T.; Tsuha, C. Energy Pile and Ground Temperature Response to Heating Test: A Case Study in Brazil. *Bulg. Chem. Commun.* **2016**, *48*, 115.

39. Hillel, D. *Introduction to Environmental Soil Physics*; Academic Press: Cambridge, MA, USA, 2003.
40. Mimouni, T.; Laloui, L. Towards a Secure Basis for the Design of Geothermal Piles. *Acta Geotech.* **2013**, *9*, 355–366. [[CrossRef](#)]
41. Suryatriyastuti, M.E.; Mroueh, H.; Burlon, S. Understanding the Temperature-Induced Mechanical Behaviour of Energy Pile Foundations. *Renew. Sustain. Energy Rev.* **2012**, *16*, 3344–3354. [[CrossRef](#)]
42. You, S.; Cheng, X.; Yu, C.; Dang, Z. Effects of Groundwater Flow on the Heat Transfer Performance of Energy Piles: Experimental and Numerical Analysis. *Energy Build.* **2017**, *155*, 249–259. [[CrossRef](#)]